Non-radial fluid oscillations of strange, hadronic and hybrid stars

L. Tonetto Coimbra[1] and G. Lugones[1]
[1] *Universidade Federal do ABC, Centro de Ciências Naturais e Humanas, Avenida dos Estados 5001- Bangú, CEP 09210-580, Santo André, SP, Brazil.*

One of the main reasons to study the internal structure of neutron stars is to connect astrophysical observations and microphysical aspects of dense matter, a fact that has increasingly attracted the scientific community attention. The study of compact objects is also interesting regarding the emission of gravitational waves, since the detection of it is something totally feasible today, as shown by the event GW150914 detected by Laser Interferometric Gravitational Wave Observatory (LIGO). Combining these two subjects relative to neutron stars, we study non-radial oscillations of strange, hadronic and hybrid non-rotating stars in the Cowling approximation. Our focus is to analyze NS models with maximum masses above the mass of the recently observed pulsars PSR J1614-2230 and PSR J0348-0432 with $M \approx 2M_{\odot}$. For hadronic EoSs we employ two different parametrizations (GM1 and NL3) of the same relativistic mean-field model and one based on Skyrme effective interactions (SLy4). For quark matter, we employ a generic MIT bag model that allows to include the effect of finite quarks masses and the color superconductivity phenomenon and the Nambu-Jona-Lasinio (NJL) model for three-flavor quark matter. Our results show that the fundamental oscillation mode is sensitive to the equation of state, but it is rather difficult to distinguish hadronic, strange and hybrid stars by just observing the f-frequency because of the overlap of the curves, mainly when the masses are around 2 $M_{\odot}$.

PACS numbers: 97.60.Jd, 26.60.Kp, 97.10.Sj, 95.85.Sz

I. INTRODUCTION

The study of the internal composition of neutron stars (NSs) is a key topic on modern astrophysics. The behavior of the dense matter strongly impacts many potentially observable properties, such as the mass-radius relation, rotational properties, oscillation modes, surface temperature and the timescales of cooling and deleptonization [1]. Therefore, astronomical observations may impose constraints to the study of dense matter at a microscopic level. Big observatories, like the Five hundred meter Aperture Spherical Telescope (FAST) and the Square Kilometer Array (SKA) will be capable of finding ten times more pulsars on binary systems and millisecond pulsars than detected until today, increasing proportionally the number of compact stars' masses measurements. Moreover, X-ray satellites such as NICER and LOFT, plane to measure the radius of compact stars with great precision. These observations might give fundamental informations about the equation of state (EoS) of the dense matter.

On the other hand, a new window of observation of the universe was opened with the detection of gravitational waves (GWs) by LIGO on September 14, 2015 [2]. After this event, many other detections are expected by LIGO and the second generation GW interferometric detectors (e.g. Advanced Virgo and KAGRA [3]) including binary mergings involving NSs [4–6]. When the desired sensitivity is reached, what is expected to around 2021, such instruments will be ten times more sensitive than the first generation and will reach approximately 10^5 galaxies allowing the detection of NSs fusions at a rate of 1 per month. It is known that several oscillation modes of NSs may emit GWs [7, 8] and such sensitivity will probably allow the detection of pulsation modes of excited compact stars in binary fusions or pulsations of newborn compact objects associated with core collapse supernovae.

Nowadays, the observational evidence is not conclusive about the internal composition of compact stars because all the measured stellar properties like mass, radius and cooling time are compatible with many equations of state (EoSs) describing stars composed by purely hadronic matter, pure quark matter (strange stars) or hybrid matter (where quark matter is present only at very high densities). However, the recent discovery of the pulsars PSR J1614-2230 and PSR J0348-0432 with masses close to $2 \sim M_{\odot}$ [9, 10] and the likely existence of more massive NSs [11, 12] strengthens the idea that some kind of exotic matter might exist in such objects.

Several works have been carried out in the last four decades in order to describe the non-radial oscillatory properties of NSs [7, 13–21]; however, these works (with the exception of [21]) considered EoSs that resulted mostly in maximum stellar masses under $2M_{\odot}$, therefore inconsistent with the observation of the pulsars PSR J1614-2230 and PSR J0348-0432. Thus, it's important to re-analyze the oscillation spectra because changing the EoS may bring new ways to distinguish hadronic stars, strange stars and hybrid stars.

In this work we study the fundamental mode of non-radial oscillations for strange, hadronic and hybrid stars considering the Cowling approximation [22]. For quark matter, we consider a Nambu-Jona-Lasinio (NJL) model found in Ref. [23] and a generic MIT bag model that allow us to analyze, e.g., the color superconductivity phenomenon and the effects of finite strange quark mass. For hadronic EoSs, we employ two different parametrizations GM1 and NL3 [24, 25] of the same relativistic mean-field

model and a model based on Skyrme effective interactions, SLy4 [26].

The paper is organized as follows: in Sec. II we describe the EoSs used for quark and hadronic matter. In Sec. III, the equilibrium stellar model employed in this work is discussed, including the mass-radius relation for the EoSs adopted. In Sec. IV, we present a brief review of the formalism of non-radial oscillations in compact stars within the Cowling approximation. In Sec. V, we present our results and in Sec. VI we discuss the main conclusions of the work. We consider $c = G = \hbar = 1$, unless explicitly stated.

II. EQUATIONS OF STATE

The exact internal composition of NSs is unknown, but we know it might be made by high density baryonic matter. Due to this uncertainty, several EoSs are used in order to confront the observational evidence. The main hypothesis for a NS interior is that matter is highly degenerate and at thermodynamic equilibrium, so that temperature effects can be neglected [27]. With these conditions, the EoS becomes one-parameter dependent: $\rho(n_B)$, $p(n_B)$ or $\rho(p)$, where ρ is the energy density, p the pressure and n_B the baryon number density.

The only analytical EoS in this paper is the MIT EoS, as will be explained soon. The other EoSs are given in tables obtained in previous works, so it is necessary to interpolate between their data to extract the necessary information. We implemented a linear interpolation formula presented on page 107 of Ref. [28].

A. Hadronic phase

The relativistic mean-field theory is widely used to describe hadronic matter in compact stars. In this work we employ the following standard Lagrangian [24, 25]:

$$\begin{aligned}\mathcal{L}_H &= \sum_B \bar{\psi}_B[\gamma_\mu(i\partial^\mu - g_{\omega B}\omega^\mu - \frac{1}{2}g_{\rho B}\vec{\tau}.\vec{\rho}^\mu) \\ &- (m_B - g_{\sigma B}\sigma)]\psi_B + \frac{1}{2}(\partial_\mu\sigma\partial^\mu\sigma - m_\sigma^2\sigma^2) \\ &- \frac{1}{4}\omega_{\mu\nu}\omega^{\mu\nu} + \frac{1}{2}m_\omega^2\omega_\mu\omega^\mu - \frac{1}{4}\vec{\rho}_{\mu\nu}.\vec{\rho}^{\mu\nu} \\ &+ \frac{1}{2}m_\rho^2\vec{\rho}_\mu.\vec{\rho}^\mu - \frac{1}{3}bm_n(g_\sigma\sigma)^3 - \frac{1}{4}c(g_\sigma\sigma)^4 \\ &+ \sum_L \bar{\psi}_L[i\gamma_\mu\partial^\mu - m_L]\psi_L, \end{aligned} \quad (1)$$

for matter composed by nucleons and electrons. Leptons L are treated as non-interacting and baryons B are coupled to the scalar meson σ, the isoscalar-vector meson ω_μ and the isovector-vector meson ρ_μ. For more details about the EoS obtained from the above Lagrangian, see [29] and references therein. There are five constants in the model that are fitted to the bulk properties of nuclear matter [25]. In this paper we use two different parametrizations shown in Table I. At low densities we use the Baym, Pethick and Sutherland (BPS) model [30] and the transition pressure is determined by the Gibbs criterion (the Gibbs free energy per baryon of the two phases is equal at the transition pressure) [31]. More details about this criterion will be given in the discussion about hybrid stars.

TABLE I: Coupling constants for the parametrizations GM1 [25] and NL3 [32].

Set	GM1	NL3
m_σ (MeV)	512	508.194
m_ω (MeV)	783	782.501
m_ρ (MeV)	770	763
g_σ	8.91	10.217
g_ω	10.61	12.868
g_ρ	8.196	8.948
b	0.002947	0.002055
c	-0.001070	-0.002651

The SLy4 EoS is based on the effective nuclear interaction SLy (Skyrme Lyon) of the Skyrme type and for further details the reader is referred to, e.g., [26] and references therein. For densities $\rho < \rho_{ND} = 4.3 \times 10^{11}\mathrm{g/cm^3}$, we adopted the HP94 EoS [33] as did in ref. [26].

B. Quark phase

For the quark phase, we use a generic MIT bag model EoS and the Nambu-Jona-Lasinio model. The first is presented in Ref. [34] with free parameters B, a_2 and a_4, which could describe several physical aspects. The model is defined by the following grand thermodynamic potential [34]

$$\Omega = -\frac{3}{4\pi^2}a_4\mu^4 + \frac{3}{4\pi^2}a_2\mu^2 + B + \Omega_e \quad (2)$$

where $\mu = (\mu_u+\mu_d+\mu_s)/3$ is the quark chemical potential and Ω_e is the grand thermodynamic potential for the electrons e. Considering a core made by quarks, we can neglect the thermodynamic contribution of the electrons there, because of the following reason. Applying local charge neutrality, we have $\frac{2}{3}n_u - \frac{1}{3}n_d - \frac{1}{3}n_s = n_e$, where n_i is the number density of the ith particles involved. From the chemical equilibrium, $\mu_d = \mu_u + \mu_e$ and $\mu_s = \mu_d$, thus we get at zero temperature the relation [34, 35]:

$$\mu_e = m_s^2/(4\mu) - m_s^4/(48\mu^3) + \mathcal{O}(m_s^6/\mu^5) \quad (3)$$

so $\mu_e/\mu \sim m_s^2/\mu^2$. The influence of electrons in quark matter can be estimated by $\Omega_e/\Omega \sim \mathcal{O}(\mu_e^4/\mu^4) \sim \mathcal{O}(m_s^8/\mu^8)$. Concerning the core of a hybrid star or a

strange star, the quark matter EoS is at the high density regime where μ is significantly larger than m_s (typically, $\mu \sim 300$ MeV and $m_s \sim 100$ MeV) . Therefore, the thermodynamic contribution of the electrons is small to the EoS and then to macroscopic stellar properties [35]. Thereby, we neglect the electron's contribution in Eq. (2) for the star core. Regarding the star's crust of strange stars, more care is necessary. Since μ is not significantly larger than m_s, we can not discard the electron's role in thermodynamic quantities. However, for this work, we assume that even for the strange stars' crust, this approximation is valid, but, emphasizing that it's worth studying this topic more carefully.

The above phenomenological model is interesting because it permits to explore many factors. The parameter a_4 ranges between $0 \leq a_4 \leq 1$, where $a_4 = 1$ indicates an ideal gas. If we consider the Quantum Chromodynamics (QCD) corrections, $a_4 \neq 1$ [34]. According to Ref. [34], a reasonable value is $a_4 \approx 0,7$. We get the standard MIT bag model setting $a_4 = 1$ and $a_2 = m_s^2$. The influence of strong interactions on the star can be studied by varying a_4 and the effect of the color superconductivity phenomenon in the Color Flavor Locked (CFL) phase can be explored setting $a_2 = m_s^2 - 4\Delta^2$, being Δ the energy gap associated with the quark pairing [34, 35]. The bag constant B is related to the confinement of the quarks, representing in a phenomenological way the vacuum energy [36].

Working with Eq. (2), it is possible to obtain a relation $p(\rho)$ or $\rho(p)$ which is necessary to solve the stellar structure equations (see below). Firstly, we have to get the pressure as a function of the chemical potential by $p = -\Omega$. The baryon number density n_B is calculated by:

$$n_B = -\frac{1}{3}\frac{\partial \Omega}{\partial \mu} = \frac{1}{\pi^2}a_4\mu^3 - \frac{1}{2\pi^2}a_2\mu. \tag{4}$$

Using the thermodynamic relation $\Omega = \rho - 3\mu n_B$, we have

$$\rho = \Omega + 3\mu n_B = -p + 3\mu n_B. \tag{5}$$

Replacing (4) in (5),

$$\rho = \frac{9}{4\pi^2}a_4\mu^4 - \frac{3}{4\pi^2}a_2\mu^2 + B, \tag{6}$$

then, solving (6) for μ^2, one obtains

$$\mu^2 = \frac{1}{2}\left[\frac{a_2 + a_2\sqrt{1 + \frac{16\pi^2 a_4}{a_2^2}(\rho - B)}}{3a_4}\right]. \tag{7}$$

Finally, linking (7) with (2) and $p = -\Omega$, we arrive to

$$p(\rho) = \frac{1}{3}(\rho - 4B) - \frac{a_2^2}{12\pi^2 a_4}\left[1 + \sqrt{1 + \frac{16\pi^2 a_4}{a_2^2}(\rho - B)}\right]. \tag{8}$$

On the other hand, depending on the values of a_2, a_4 and B, either hybrid stars or strange stars may exist. The former only exist if the transition pressure is greater than zero. In this paper, it is assumed that the interface between hadrons and quarks is a sharp discontinuity determined by Gibbs condition where $p_{quarks} = p_{hadrons}$ and $g_{quarks} = g_{hadrons}$, being $g = (\rho + p)/n_B = 3\mu$ the Gibbs free energy per baryon [31, 35]. The quark-hadron interface will be located at $p > 0$ only if $B > B_{min}$ for given values of a_2 and a_4 [35]:

$$B_{min} = \frac{g^2(0)}{108\pi^2}[g^2(0)a_4 - 9a_2], \tag{9}$$

where $g(0)$ is the Gibbs free energy per baryon at null pressure. By the Gibbs condition, $g(0)$ is the energy per baryon of pressureless hadronic matter, which we consider to be that of the iron, approximately 930 MeV.

However, we also need that the hadronic phase in a hybrid star is not in metastable equilibrium, i.e. the ud deconfined quark matter, must be less energetically favorable than hadronic matter composed by protons and neutrons, thus $g_{ud}(0) > 930$ MeV. For ud quark matter without electrons and in the massless limit, one has that [35]

$$\Omega_{2f} = -\tilde{p} = -\frac{24a_4}{4\pi^2(1 + 2^{1/3})^3}\tilde{\mu}^4 + \frac{2a_2}{4\pi^2}\tilde{\mu}^2 + B, \tag{10}$$

where $\tilde{\mu} \equiv (\mu_u + \mu_d)/2 = (1 + 2^{1/3})\mu_u$ (due to local charge neutrality). From $\tilde{n}_b = -\frac{1}{3}(\partial\Omega_{2f}/\partial\tilde{\mu})$ and $\tilde{\epsilon} = -\tilde{p} + n_u\mu_u + n_d\mu_d = -\tilde{p} + 3\tilde{n}_b\tilde{\mu}$, one has the 2-flavor stability condition $B > \tilde{B}_{min}$, where [35]

$$\tilde{B}_{min} = \frac{g^2(0)}{54\pi^2}\left[\frac{4g^2(0)a_4}{(1 + 2^{1/3})^3} - 3a_2\right]. \tag{11}$$

Figure 1 of Ref. [35] clarifies the issue of stability with a plot delimiting regions for absolutely stable strange stars and hybrid stars in a $(B^{1/4}, a_4)$ plane. In view of this discussion, we assume for MIT strange stars the values of the parameters contained in Table II. In this table, we consider $a_2^{1/2} = 100$ MeV, in order to explore Figure 1 of Ref. [35]. We also build hybrid stars with this EoS, but with different parameter sets, as will be explained in the next subsection.

The other quark EoS used in this work is the SU(3) NJL model with scalar-pseudoscalar, isoscalar-vector and 't Hooft six fermion interaction, which is present in ref. [23]. The Lagrangian density of the model is [23]:

$$\begin{aligned}
\mathcal{L}_Q &= \bar{\psi}(i\gamma_\mu\partial^\mu - \hat{m})\psi \\
&+ g_s\sum_{a=0}^{8}[(\bar{\psi}\lambda^a\psi)^2 + (\bar{\psi}i\gamma_5\lambda^a\psi)^2] \\
&- g_v\sum_{a=0}^{8}[(\bar{\psi}\gamma_\mu\lambda^a\psi)^2 + (\bar{\psi}\gamma_5\gamma_\mu\lambda^a\ \psi)^2] \\
&+ g_t\{\det[\bar{\psi}(1+\gamma_5)\psi] + \det[\bar{\psi}(1-\gamma_5)\psi]\},
\end{aligned} \tag{12}$$

TABLE II: Parameters a_2, a_4 and B for strange stars within the MIT bag model EoS.

Set	$B^{1/4}$[MeV]	a_4	$a_2^{1/2}$[MeV]
MIT1	119	0.5	100
MIT2	122	0.5	100
MIT3	127	0.5	100
MIT4	132	0.7	100
MIT5	136	0.7	100
MIT6	141	0.7	100
MIT7	141	0.9	100
MIT8	146	0.9	100
MIT9	152	0.9	100

being $\psi = (u, d, s)$ the quark fields, $\lambda^a (0 \leq a \leq 8)$ the SU(3) flavor matrices, $\hat{m} = \mathrm{diag}(m_u, m_d, m_s)$ the quark current mass, and g_s, g_v and g_t coupling constants. The mean-field thermodynamic potential density Ω for a given baryon chemical potential μ at $T = 0$, is given by

$$\begin{aligned}\Omega = & - \eta N_c \sum_i \int_{k_{Fi}}^{\Lambda} \frac{p^2\, dp}{2\pi^2} \sqrt{p^2 + M_i^2} + 2g_s \sum_i \langle\bar{\psi}\psi\rangle_i^2 \\ & - 2g_v \sum_i \langle\psi^\dagger\psi\rangle_i^2 + 4g_t \langle\bar{u}u\rangle\langle\bar{d}d\rangle\langle\bar{s}s\rangle \\ & - \eta N_c \sum_i \mu_i \int_0^{k_{Fi}} \frac{p^2\, dp}{2\pi^2} - \Omega_0, \end{aligned} \tag{13}$$

where the sum is over the quark flavor ($i = u, d, s$), the constants $\eta = 2$ and $N_c = 3$ are the spin and color degeneracies, and Λ is a regularization ultraviolet cutoff to avoid divergences in the medium integrals. The Fermi moment of the particle i is given by $k_{Fi} = \theta(\mu_i^* - M_i)\sqrt{(\mu_i^{*2} - M_i^2)}$, where μ_i^* is the quark chemical potential modified by the vectorial interaction, i.e. $\mu_{u,d,s}^* = \mu_{u,d,s} - 4g_v\langle\psi^\dagger\psi\rangle_{u,d,s}$. All the parameters used in this paper are the same as in Ref. [23]. Also, as in Ref. [23], g_v is treated as a free parameter by the fact that the masses of the vector mesons are not dictated by chiral symmetry. To obtain the EoS, it was assumed that matter is charge neutral and in equilibrium under weak interactions [23].

The treatment for the Ω_0 term assumed in this paper is the same as in Ref. [23]. Then, here we also explore the influence of a change $\Omega_0 \longrightarrow \Omega_0 + \delta\Omega_0$ in the macroscopic properties of compact stars. It is important to note that, for this NJL parametrization, it is not possible to build strange stars [23], so we just use it for hybrid stars.

C. Hybrid matter

For hybrid stars, we combine the MIT and the NJL EoSs with the NL3 EoS. In the case MIT+NL3, we use $a_4 = 0.5$ and $B^{1/4} = 135$, 136, 137,...,145 MeV for $a_2^{1/2} = 100$ MeV and $a_2^{1/2} = 150$ MeV. The motivation to use $a_2^{1/2} = 100$ MeV and the cited values of a_4 and $B^{1/4}$ is to compare with the results of Ref. [37]. We also use $a_2^{1/2} = 150$ MeV in order to analyze the influence of a_2 in the star's stability and maximum mass. Regarding NJL+NL3, we use $g_v/g_s = 0.1$, 0.2, 0.3 for $\delta\Omega_0 = 0$ and $g_v/g_s = 0.2$, 0.3, 0.4 for $\delta\Omega_0 = -10$ MeV/fm^3 and $\delta\Omega_0 = -15$ MeV/fm^3. These parameters are adopted in order to obtain stable configurations with $M_{max} \gtrapprox 2\, M_\odot$, as in Ref. [23]. The phase transition pressure is obtained by the Gibbs condition $g_{tran} = g_{quarks} = g_{hadrons}$ at $p_{tran} = p_{quarks} = p_{hadrons}$, where $g = (\rho + p)/n_B$, for all hybrid stars [31].

III. STELLAR STRUCTURE EQUATIONS

The compact star's equilibrium structure must be taken into account to calculate non-radial oscillations. We assume that compact objects are made of layers of perfect fluids, whose stress-energy tensor is

$$T_{\mu\nu} = (\rho + p)u_\mu u_\nu + p g_{\mu\nu}, \tag{14}$$

where u^μ is the fluid's four-velocity and $g_{\mu\nu}$ is the metric. We also set a spherically symmetric background spacetime for the whole star given by the line element

$$ds^2 = -e^{2\nu(r)}dt^2 + e^{2\lambda(r)}dr^2 + r^2(d\theta^2 + \sin^2\theta d\phi^2), \tag{15}$$

where $\nu(r)$ and $\lambda(r)$ are metric functions with respect to r. A mass function $m(r)$ is defined as $m(r) = r(1 - e^{-2\lambda})/2$ [31]. Solving Einstein's equations, we get the stellar structure equations (Tolman-Oppenheimer-Volkoff (TOV) equations [38])

$$\frac{dp}{dr} = \frac{-(\rho(r) + p(r))(m(r) + 4\pi p(r) r^3)}{r(r - 2m(r))}, \tag{16}$$

$$\frac{d\nu}{dr} = -\frac{1}{\rho(r)}\frac{dp}{dr}\left(1 + \frac{p(r)}{\rho(r)}\right)^{-1}, \tag{17}$$

$$\frac{dm}{dr} = 4\pi r^2 \rho(r), \tag{18}$$

where $m(r)$ is the gravitational mass inside r, as measured in a proper frame of reference, and t, r, θ, ϕ form the Schwarzschild coordinate system. It is necessary an EoS $p(\rho)$ to close the system of equations. The boundary conditions are

$$m(r = 0) = 0, \tag{19}$$

$$p(r = R) = 0, \tag{20}$$

$$\nu(r = R) = \frac{1}{2}\ln\left(1 - \frac{2M}{R}\right), \tag{21}$$

being R the radius of the star and $M = m(R)$. The condition of Eq. (21) is necessary for the metric function $\nu(r)$ smoothly match the Schwarzschild metric outside the star [39].

The TOV equations form a set of first order differential equations. The integration of them is made by using a 5^{th} order Runge-Kutta method with an adaptive step, which is explained in Sec. 16.2 of Ref. [28]. Besides that, it is important to notice that the TOV equations have a singularity at $r = 0$, so we have to start the integration at a radius slightly larger than 0, e.g. 1 meter. To find m, ν and p at this new point, we have to make a Taylor series expansion around $r = 0$, as shown in Ref. [40].

Additionally, ν is not defined at $r = 0$. In order to match the boundary condition given in Eq. (21), we start the integration for an arbitrary value of ν and then, after the star's surface is reached, subtract $\nu(R)$ and add $\frac{1}{2}\ln(1-\frac{2M}{R})$ to all the values of ν through the star. Therefore, Eq. (21) is satisfied and $\nu(r)$ is corrected all over the star [39].

In view of the observations of the massive pulsars PSR J1614-2230 with $M = (1.97 \pm 0.04)M_\odot$ [9] and PSR J0348-0432 with $M = (2.01 \pm 0.04)M_\odot$ [10], the EoSs of most interest for us are those that can build neutron stars with $M \gtrapprox 2M_\odot$. In order to know the maximum stellar mass for each EoS, we solve the equations (16) and (18) considering several values of central pressure and save the maximum mass for each of them. With these points, we plot the mass-radius relation for each EoS.

Figure 1 shows the mass-radius relations for all stellar models used in this work. The horizontal black solid line corresponds to $M = 2.01\ M_\odot$, the measured mass of pulsar PSR J0348-0432, which is shown to visualize the EoSs that produce maximum stellar masses above this value. From these plots, we see that most models allow $M_{max} \gtrapprox 2\ M_\odot$. From panel (a) of Fig. 1, one notices that there are only two NJL+NL3 sets that have $M < 2.01\ M_\odot$: ($\delta\Omega_0 = -15$ MeVfm^{-3}, $g_v/g_s = 0.2$) and ($\delta\Omega_0 = 0$, $g_v/g_s = 0.1$). The maximum masses obtained here are equivalent to those presented in Ref. [23]. The $M - R$ curves show a bend when they become hybrid and in this transition we check the stellar stability. The hadronic part of a mass-radius plot characterizes a stable configuration, so, according to the stability criterion shown in Sec. 6.8 of Ref. [31], if dM/dR changes signal at a critical point, the stability changes. Thus, we can identify if a given combination of a quark matter EoS and an hadronic EoSs can generate stable hybrid stars with a sufficiently large maximum mass.

In panel (a) of Fig. 1, all the sets have stable hybrid branches, except ($\delta\Omega_0 = 0$,$g_v/g_s = 0.3$), however, as said before, ($\delta\Omega_0 = -15$ MeVfm^{-3}, $g_v/g_s = 0.2$) and ($\delta\Omega_0 = 0$, $g_v/g_s = 0.1$) do not have $M_{max} \geq 2.01\ M_\odot$. The stable hybrid branch of ($\delta\Omega_0 = -10$ MeVfm^{-3}, $g_v/g_s = 0.4$) is almost imperceptible.

Panels (b) and (d) of Fig. 1 show the mass-radius plot for hybrid stars combining MIT+NL3, for $a_2^{1/2} = 100$ MeV and $a_2^{1/2} = 150$ MeV, respectively, keeping $a_4 = 0.5$ and varying B. For $a_2^{1/2} = 100$ MeV, all the curves have a maximum mass above 2.01 $M_\odot$ and also have a large hybrid branch. This was expected, in view of the results of Ref. [37]. Setting $a_2^{1/2} = 150$ MeV, all curves also have maximum mass above 2.01 $M_\odot$, but the stable hybrid branch is greatly reduced, therefore, we can expect less stable configurations raising a_2. All of them, except for $B^{1/4} = 142$ MeV, have stable hybrid stars. From Eq. (2) in the case of unpaired three-flavor quark matter, we note that $a_2^{1/2}$ corresponds to m_s, so, increasing m_s in this particular case, the stability decreases.

At panel (c) of Fig. 1, we show the mass-radius relations for strange and hadronic stars, where we fix $a_2^{1/2} = 100$ MeV and vary B and a_4. From this plot, it is possible to conclude that increasing B, the maximum mass decreases and, for fixed B, a larger a_4 implies a larger maximum mass.

IV. NON-RADIAL FLUID MODES FOR COMPACT STARS

Quadrupole oscillations of compact stars emit gravitational waves (GWs). The oscillations are damped as the GWs carry out their energy. Such oscillations are called quasinormal modes (QNMs) [22]. These modes have complex frequencies, whose imaginary part represents the damping rate and the real part the oscillation frequency, analogous to electromagnetic waves. They are divided in two categories: fluid modes and spacetime modes. The first is split in f, p and g modes for non-rotating stars and the latter in w and w_{II} modes (there exist also the so called trapped modes for spacetime modes, but they are not compatible with well known EoSs) [22]. In this work we focus on f modes, so we briefly explain the fluid modes below:

- f-mode (fundamental mode): there exist just one f mode for each l (from the spherical harmonic Y_{lm}). According to Ref. [41], the eigenfunction for this mode does not have nodes inside the star and decays from the star's center to the surface. The typical value of the f frequency for a neutron star is 1.5−3 kHz [22];
- p-mode (pressure or acoustic mode): the restoring force is caused by the pressure gradient inside the star. They are labeled as p_1, p_2, p_3,..., p_∞ in order from the lower to the higher frequency. They strongly depend on the star composition. The p_1 typical oscillation frequency for a neutron star is $4 - 7$kHz;
- g-mode (gravity mode): this mode arises from a gravitational field discontinuity, e.g., a density discontinuity. They are labeled as g_1, g_2, g_3,..., g_∞ in order from the higher to the lower frequency. The typical oscillational frequency is less than 100 Hz.

The formalism for studying non-radial modes within the theory of General Relativity was treated in the pioneering work of Thorne and Campollataro [42] and further extended by other authors (see [13] and references

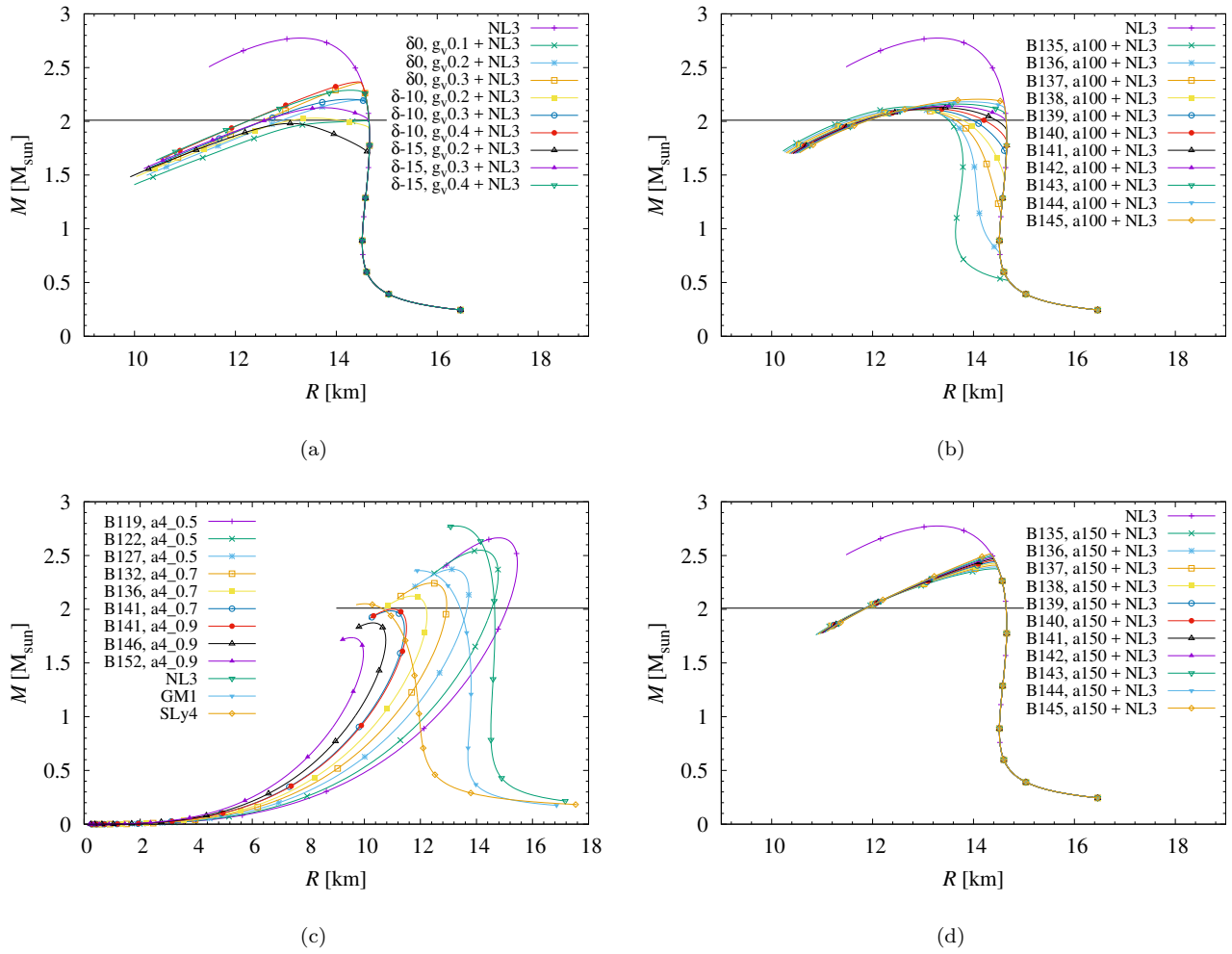

FIG. 1: (a) Mass-radius plot for hybrid stars using NJL+NL3, where the labels indicate the value of $\delta\Omega_0$ in MeV fm^{-3} and the ratio g_v/g_s. (b) Mass-radius graphic for hybrid stars using MIT+NL3 fixing $a_4 = 0.5$, where the labels indicate the value of $a_2^{1/2}$ in MeV and $B^{1/4}$ in MeV. (c) Mass-radius plot for strange and hadronic stars, fixing $a_2^{1/2} = 100$ MeV, where the labels indicate the values of a_4 and $B^{1/4}$ in MeV. (d) Same caption as (b).

therein). The perturbation equations are decomposed into spherical harmonics leading to two classes of oscillations according to the parity of the harmonics. Even (or polar) oscillations produce spheroidal deformations on the fluid, while odd (or axial) oscillations produce toroidal deformations (see e.g Kokkotas and Schmidt [8] and references therein) [21]. For non-rotating stars composed of a perfect fluid, the fluid axial oscillations lead to a zero frequency trivial solution to the perturbation equations with vanishing pressure and density variations while the space-time axial modes (w-modes or w_{II}-modes) are of non-zero frequency [21].

For polar oscillations the linearised field equations inside the star can be written as a system of three wave equations, where two of them correspond to the perturbations of the space-time and the other one to the density perturbations inside the star [8]. If the gravitational field is very weak, we can neglect the two equations corresponding to the metric perturbation and we only remain with the one describing the fluid oscillations. This approach is known as the Cowling approximation and considerably simplifies the analysis. This method was first introduced by the Ref. [41] for the study of Newtonian stars and subsequently adapted by Ref. [43] for the investigation of relativistic stars [21].

For typical relativistic stars, recent studies show that the oscillation frequencies calculated by the complete linearised equations of general relativity and by the Cowling approximation differ by less than 20 % for f-modes, around 10% for p-modes [14] and less than a few percent for g-modes [16]. This justifies its wide utilization for studying, e.g., slowly and differentially rotating compact stars [44], rapidly rotating relativistic stars consisting of a perfect fluid obeying a polytropic equation of state (EoS) [45], elastic modes of oscillation in the crust of a neutron star [46] and neutron stars with internal anisotropic pres-

sure [47]. In this work we employ the pulsation equations within the Cowling approximation as derived by [20]. To obtain these equations, fluid perturbations are decomposed into spherical harmonics $Y_{lm}(\theta,\phi)$ and a sinusoidal time dependence $\exp(i\omega t)$ with frequency ω. The Lagrangian fluid displacements that represent the infinitesimal oscillatory perturbations of the star are [21]

$$\xi^i = \left(e^{-\Lambda}W, -V\partial_\theta, -V\sin^{-2}\theta\partial_\phi\right) r^{-2}Y_{\ell m}e^{i\omega t}, \quad (22)$$

being W and V functions of r. The pulsation equations read:

$$W' = \frac{d\rho}{dp}\left[\omega^2 r^2 e^{\Lambda-2\Phi}V + \Phi' W\right] - \ell(\ell+1)e^{\Lambda}V, \quad (23)$$

$$V' = 2\Phi' V - e^{\Lambda}\frac{W}{r^2}. \quad (24)$$

where primes denote the derivatives with respect to r [20]. To close the system we need boundary conditions at the center ($r = 0$) and at the surface ($r = R$) of the star. The behaviour of W and V near the center of the star can be obtained from the above equations and is given by $W(r) = Cr^{\ell+1} + \mathcal{O}(r^{\ell+3})$ and $V(r) = -Cr^{\ell}/\ell + \mathcal{O}(r^{\ell+2})$, where C is an arbitrary constant. At the surface of the star the Lagrangian perturbation in the pressure must be zero ($\Delta p = 0$), leading to [21]

$$\omega^2 r^2 e^{\Lambda-2\Phi}V + \Phi' W = 0. \quad (25)$$

In the case of hybrid stars, we have to impose additional junction conditions at the density discontinuity between the quark and the hadronic phases. These junction conditions are [20]

$$W_+ = W_-, \quad (26)$$

$$V_+ = \frac{e^{2\Phi}}{\omega^2 {R_g}^2}\Big(\frac{\rho_- + p}{\rho_+ + p}\left[\omega^2 {R_g}^2 e^{-2\Phi}V_- + e^{-\Lambda}\Phi' W_-\right] - e^{-\Lambda}\Phi' W_+\Big), \quad (27)$$

where R_g represents the position of the density discontinuity, and the values of W, V, and ρ at both sides of the discontinuity are denoted by: $W_- \equiv W(R_g - 0)$, $V_- \equiv V(R_g - 0)$, $\rho_- \equiv \rho(R_g - 0)$, $W_+ \equiv W(R_g + 0)$, $V_+ \equiv V(R_g + 0)$, and $\rho_+ \equiv \rho(R_g + 0)$ [20–22]. Notice that we have to solve the TOV equations before (23) and (24) in order to store the variables that we need all over the star.

One way to solve the oscillation equations for hadronic stars and hybrid stars, i.e., without the junction conditions of equations (26) and (27) is the *shooting method*, which is a procedure to solve boundary value problems. For example: if we want to integrate a system of three dependent variables y_1, y_2 e y_3, starting from a point x_1 up to a point x_2, with a boundary condition for y_1 at x_1 and two conditions for y_2 and y_3 at x_2. In this case, one does not have the values of y_2 and y_3 at x_1, then the integration is made by shooting values for y_2 and y_3 at x_1 till the boundary conditions at the final point are satisfied. A code implementing this algorithm is found at section 17.1 of Ref. [28]. For the oscillation equations, we give V and W at the star's center, but we do not know if they satisfy Eq. (25) at the surface, so we use the shooting method to solve this problem considering a third differential equation: $(\omega^2)' = 0$, being ω the eigenfrequency of the star. We integrate for a trial value of ω^2 and adjust it until we can match the boundary condition through a Newton-Raphson procedure. For hybrid stars, we must impose the junction conditions of equations (26) and (27). To do this, it is possible to integrate the oscillation equations up to the phase transition radius, set V and W to fulfill the junction conditions and carry out the integration till the star's surface. In order to determine the phase transition radius, it's necessary to know the phase transition pressure and integrate before the TOV equations to obtain r_{tran}.

V. RESULTS

In this work, we compute the f-mode of non-radial oscillations (ℓ =2) for strange, hadronic and hybrid stars, in order to know if it is possible to gain some information about the star's internal composition looking to the f-frequency. Regarding strange stars, we use the MIT bag model of Eq. (2); for hadronic stars, we use the GM1 and NL3 parametrizations related to the Lagrangian of Eq. (1) and a Skyrme effective interaction model SLy4; for hybrid stars, we combine the NJL (Eq. (13)) and the MIT models with the NL3 EoS.

Figure 2 shows the f-frequency for hybrid, strange and hadronic stars. As in Fig. 1, it is apparent when hybrid matter takes place: there is a folding in the curve at the mass value when the quark core takes place.

In panel (a) we present the f-frequency as a function of stellar mass for hybrid stars combining NJL+NL3. Looking just to the f-mode spectrum, it would be hard to distinguish any information about the values of $\delta\Omega_0$ and g_v/g_s, because the curves overlap in many regions, but we see that for a fixed $\delta\Omega_0$, increasing g_v/g_s implies a smaller mass where the quark core appears. This conclusion can be drawn by Fig. 1 too.

Regarding panel (b), as shown by Fig. 1, a small change in $B^{1/4}$ induces a significant change in the mass where the core arises. However, by the fact of the f-mode curve be barely steep, it is still hard to differentiate possible values of parameters of the MIT model. Around 2.2 $M_\odot$, we see that all the curves overlap.

In panel (d), differentiating hybrid stars with different B is more difficult than when we set $a_2^{1/2} = 100$ MeV (panel (b)). Again, all curves overlap around 2.2 $M_\odot$.

Looking to panel (c) the situation is slightly better because strange and hadronic stars have a qualitatively different f-mode curve behavior, with the hadronic curve being steeper than the quark one. However, it remains

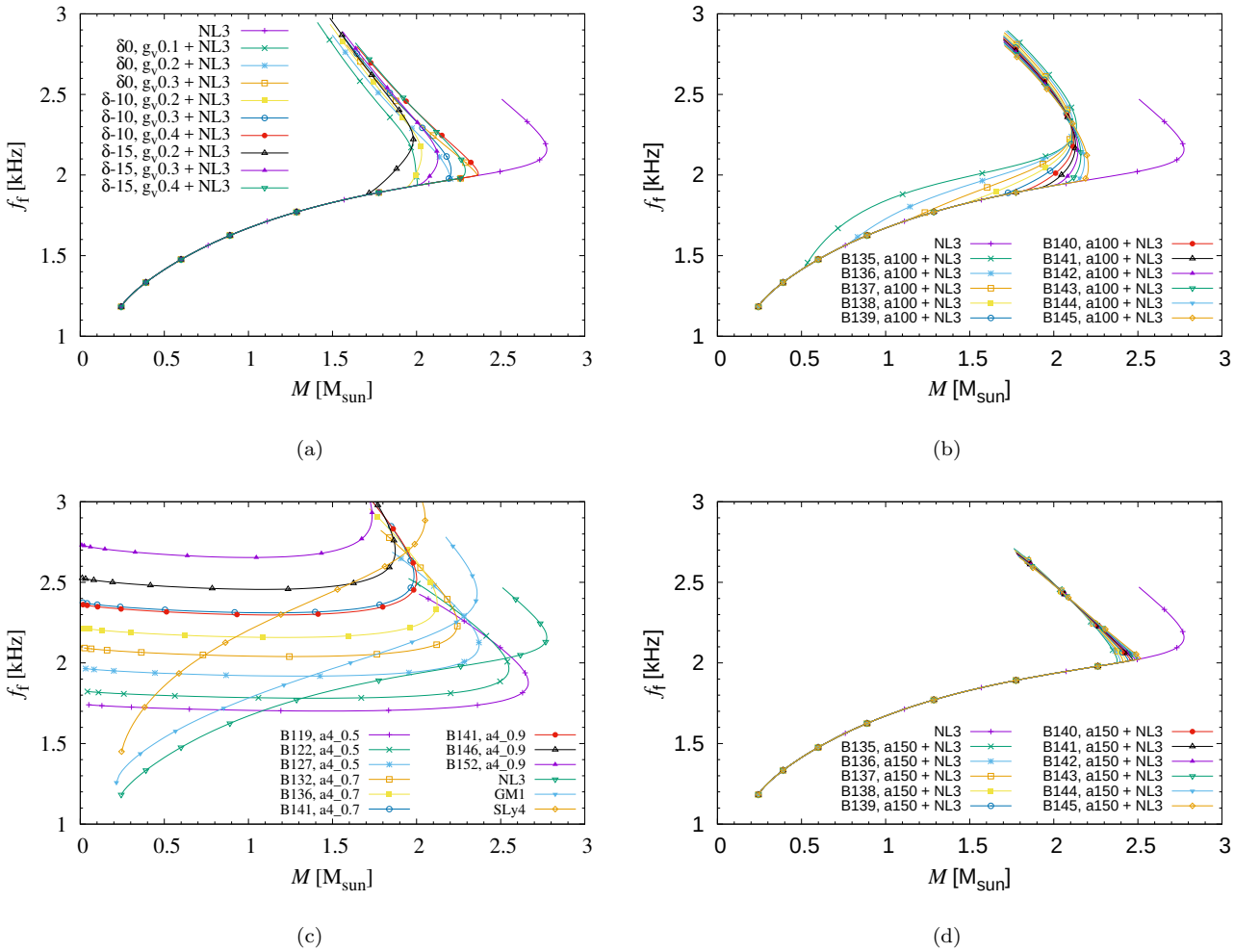

FIG. 2: (a) f-frequency for hybrid stars using NJL+NL3, where the labels indicate the value of $\delta\Omega_0$ in MeV fm^{-3} and the ratio g_v/g_s. (b) f-frequency for hybrid stars using MIT+NL3 fixing $a_4 = 0.5$, where the labels indicate the value of $a_2^{1/2}$ in MeV and $B^{1/4}$ in MeV. (c) f-frequency for strange and hadronic stars, fixing $a_2^{1/2} = 100$ MeV, where the labels indicate the values of a_4 and $B^{1/4}$ in MeV. (d) Same caption as (b).

hard to distinguish the internal composition precisely because the curves overlap in the region with large enough M, which is the relevant one from the observational point of view. If we consider the overall scenario, including the analysis of hybrid, strange and hadronic stars, all of them have a f-frequency in the range 1.5−3.5 kHz, therefore, it is rather difficult to make any affirmation about the compact star's internal composition based on these results.

VI. SUMMARY AND CONCLUSIONS

In this work we have investigated non-radial fluid oscillations of strange, hadronic and hybrid stars focusing on the f-mode. In the light of the pulsars PSR J1614-2230 and PSR J0348-0432, we have analyzed EoSs that generate maximum stellar masses above approximately 2 $M_\odot$, while briefly discussing the stability of these models. For quark matter, we have used a MIT bag model and a NJL EoSs; for hadronic matter, we employed two widely used parametrizations of a relativistic mean-field model and one based on Skyrme effective interactions. The equations of oscillation were solved within the Cowling approximation, integrated by a 5$^{\text{th}}$ order Runge-Kutta with adaptive step-size and using the *shooting method* to match the surface boundary condition.

We find that the f-mode is sensitive to the EoS employed, but, even so, it is rather difficult to distinguish hadronic, strange and hybrid stars just observing the f-frequency because of the overlap of the curves, mainly when the masses are around 2 $M_\odot$. Therefore, to obtain more (observationally) relevant conclusions, we need to analyze other oscillation modes, such as the p-mode and the g-mode. Nonetheless, the fundamental mode helps us to put some constraints on which frequency band ap-

proximately would come to the detectors.

Regarding the GWs observability, since the detection of event GW150914 by LIGO [2], many others have been detected [4–6]. Studying stellar pulsations can help us to analyze future observations of binary mergers, for example.

Finally, it is important to keep in mind that there may be other modes in the same frequency range studied here that can make even more difficult the identification of the internal composition of compact stars. Besides this, it is known that rotation changes the frequency range of the modes, although this modification would not alter qualitatively our results [48].

Acknowledgments

L. Tonetto Coimbra acknowledges the Fundação de Amparo à Pesquisa do Estado de São Paulo (FAPESP) under grant No. 2016/08412-4. G. Lugones acknowledges the Brazilian agencies Conselho Nacional de Desenvolvimento Científico e Tecnológico (CNPq) and FAPESP for financial support.

[1] G. Lugones, Eur. Phys. J. **A52**, 53 (2016), 1508.05548.
[2] B. P. Abbott, R. Abbott, T. D. Abbott, M. R. Abernathy, F. Acernese, K. Ackley, C. Adams, T. Adams, P. Addesso, R. X. Adhikari, et al., Physical Review Letters **116**, 061102 (2016), 1602.03837.
[3] K. Riles, Progress in Particle and Nuclear Physics **68**, 1 (2013).
[4] B. P. Abbott, R. Abbott, T. D. Abbott, M. R. Abernathy, F. Acernese, K. Ackley, C. Adams, T. Adams, P. Addesso, R. X. Adhikari, et al., Physical Review Letters **116**, 241103 (2016), 1606.04855.
[5] B. P. Abbott, R. Abbott, T. D. Abbott, F. Acernese, K. Ackley, C. Adams, T. Adams, P. Addesso, R. X. Adhikari, V. B. Adya, et al., Physical Review Letters **118**, 221101 (2017), 1706.01812.
[6] B. P. Abbott, R. Abbott, T. D. Abbott, F. Acernese, K. Ackley, C. Adams, T. Adams, P. Addesso, R. X. Adhikari, V. B. Adya, et al., Physical Review Letters **119**, 161101 (2017), 1710.05832.
[7] N. Andersson and K. D. Kokkotas, Monthly Notices of the Royal Astronomical Society **299**, 1059 (1998).
[8] K. D. Kokkotas and B. G. Schmidt, Living Rev. Rel **2**, 262 (1999).
[9] P. B. Demorest, T. Pennucci, S. M. Ransom, M. S. E. Roberts, and J. W. T. Hessels, Nature (London) **467**, 1081 (2010), 1010.5788.
[10] J. Antoniadis et al., Science **340**, 6131 (2013), 1304.6875.
[11] R. W. Romani et al., The Astrophysical Journal Letters **760**, L36 (2012).
[12] D. L. Kaplan et al., The Astrophysical Journal **765**, 158 (2013).
[13] S. L. Detweiler and L. Lindblom, Astrophys. J. **292**, 12 (1985).
[14] S. Yoshida and Y. Kojima, Monthly Notices of the Royal Astronomical Society **289**, 117 (1997).
[15] C. W. Yip, M.-C. Chu, and P. T. Leung, The Astrophysical Journal **513**, 849 (1999).
[16] H. Sotani, K. Tominaga, and K.-i. Maeda, Phys. Rev. D **65**, 024010 (2001).
[17] G. Miniutti, J. A. Pons, E. Berti, L. Gualtieri, and V. Ferrari, Monthly Notices of the Royal Astronomical Society **338**, 389 (2003).
[18] O. Benhar, V. Ferrari, and L. Gualtieri, Phys. Rev. D **70**, 124015 (2004).
[19] O. Benhar, V. Ferrari, L. Gualtieri, and S. Marassi, General Relativity and Gravitation **39**, 1323 (2007).
[20] H. Sotani, N. Yasutake, T. Maruyama, and T. Tatsumi, Phys. Rev. D **83**, 024014 (2011).
[21] G. Lugones and C. V. Flores, Classical and Quantum Gravity **31**, 155002 (2014).
[22] H. Sotani, Ph.D. thesis, Waseda University (2004).
[23] C. H. Lenzi and G. Lugones, Astrophys. J. **759**, 57 (2012), 1206.4108.
[24] J. Boguta and A. R. Bodmer, Nuclear Physics A **292**, 413 (1977).
[25] N. K. Glendenning and S. A. Moszkowski, Phys. Rev. Lett. **67**, 2414 (1991).
[26] F. Douchin and P. Haensel, Astron. Astrophys. **380**, 151 (2001), astro-ph/0111092.
[27] S. Bernuzzi and A. Nagar, Phys. Rev. D **78**, 024024 (2008).
[28] W. H. Press, S. A. Teukolsky, W. T. Vetterling, and B. P. Flannery, Numerical recipes in Fortran 77: The art of scientific computing (Cambridge University Press, 1997).
[29] G. Lugones, T. A. S. Do Carmo, A. G. Grunfeld, and N. N. Scoccola, Phys. Rev. D **81**, 085012 (2010), 1001.1709.
[30] G. Baym, C. Pethick, and P. Sutherland, The Astrophysical Journal **170**, 299 (1971).
[31] S. L. Shapiro and S. A. Teukolsky, Black Holes, White Dwarfs and Neutron Stars: The Physics of Compact Objects (Wiley, 2008), ISBN 9783527617678.
[32] G. A. Lalazissis, J. König, and P. Ring, Phys. Rev. C **55**, 540 (1997), nucl-th/9607039.
[33] P. Haensel and B. Pichon, Astronomy and Astrophysics **283**, 313 (1994), nucl-th/9310003.
[34] M. Alford, M. Braby, M. Paris, and S. Reddy, The Astrophysical Journal **629**, 969 (2005).
[35] J. P. Pereira, C. V. Flores, and G. Lugones (2017), 1706.09371.
[36] C. Vasquez Flores and G. Lugones, Phys. Rev. **D82**, 063006 (2010), 1008.4882.
[37] S. Weissenborn, I. Sagert, G. Pagliara, M. Hempel, and J. Schaffner-Bielich, Astrophys. J. **740**, L14 (2011), 1102.2869.
[38] J. R. Oppenheimer and G. M. Volkoff, Phys. Rev. **55**, 374 (1939), URL `http://link.aps.org/doi/10.1103/PhysRev.55.374`.
[39] N. K. Glendenning, Compact Stars: Nuclear Physics, Particle

Physics, and General Relativity (Springer, 1997).
[40] L. Lindblom and S. Detweiler, Astrophysical Journal Supplement Series **53**, 73 (1983).
[41] T. G. Cowling, Monthly Notices of the Royal Astronomical Society **101**, 367 (1941).
[42] K. Thorne and A. Campolattaro, American Physics Journal **149**, 591 (1967).
[43] P. McDermott, H. M. Van Horn, and J. Scholl, The Astrophysical Journal **268**, 837 (1983).
[44] A. Stavridis, A. Passamonti, and K. Kokkotas, Physical Review D **75**, 064019 (2007).
[45] S. Boutloukos and H.-P. Nollert, Physical Review D **75**, 043007 (2007).
[46] L. Samuelsson and N. Andersson, Monthly Notices of the Royal Astronomical Society **374**, 256 (2007).
[47] D. D. Doneva and S. S. Yazadjiev, Physical Review D **85**, 124023 (2012).
[48] E. Gaertig and K. D. Kokkotas, Phys. Rev. **D80**, 064026 (2009), 0905.0821.